

Supporting Information

The Effect of Mg-doping and Cu nonstoichiometry on the Photoresponse of CuFeO_2

Anna Wuttig, Jason W. Krizan, Jing Gu, Jessica J. Frick, Robert J. Cava
and
Andrew B. Bocarsly *

I. Ohmic Contact of $\text{CuFe}_{1-x}\text{Mg}_x\text{O}_2$ Electrodes

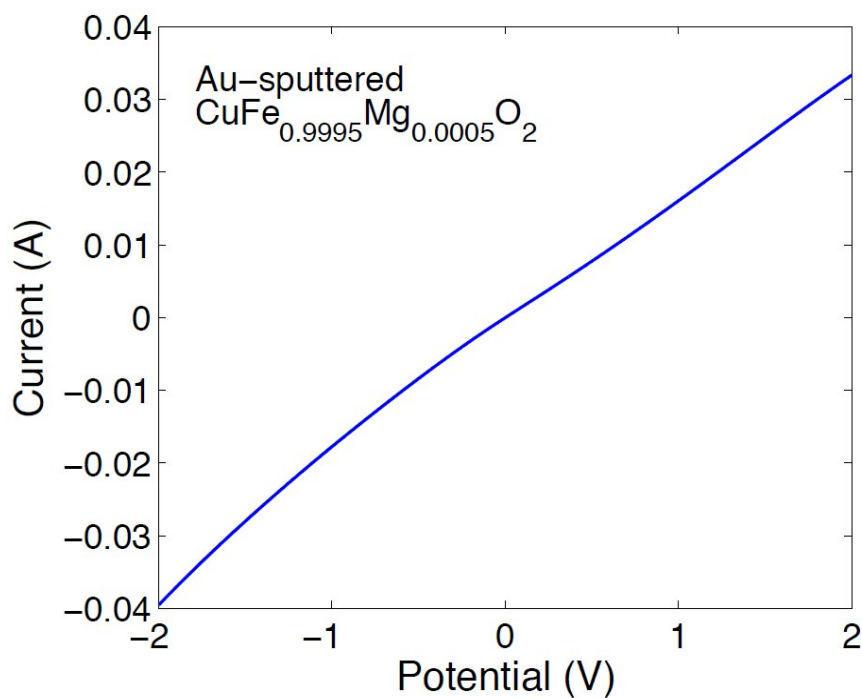


Figure S1. Representative plot of ohmic behavior for Au-sputtered $\text{CuFe}_{1-x}\text{Mg}_x\text{O}_2$, $x = 0.0005$, shown using linear sweep voltammetry. Pellet used for this measurement did not employ the densification method, thus showing high I/V resistivity in comparison to that found via the 4-point probe method. Data provided by Dr. Jing Gu from [1].

II. SEM and EDX analysis of as-synthesized CuFeO_2 pellets

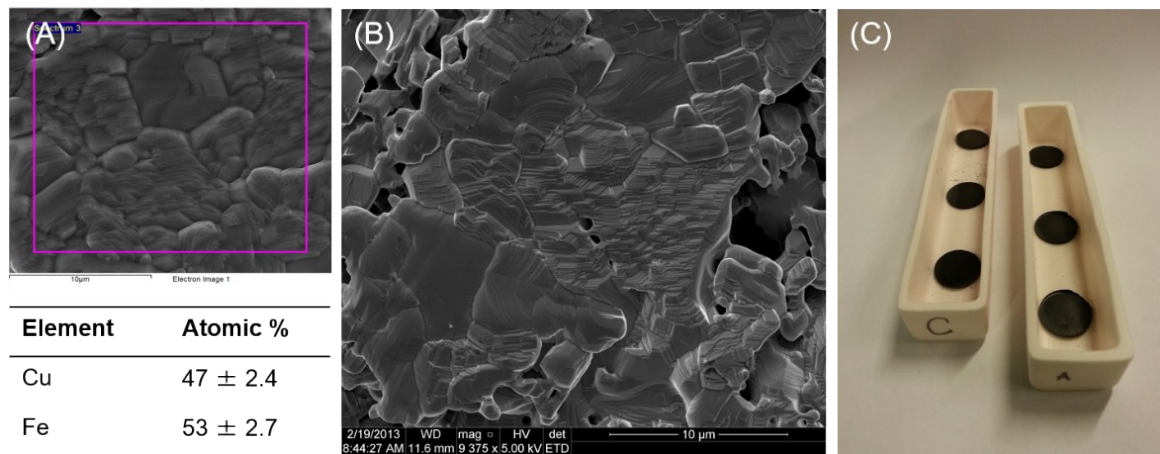


Figure S2: (A) SEM image and corresponding EDX analysis of a CuFeO_2 pellet. (B) SEM of dense CuFeO_2 pellets used in this study. (C) Photograph of pellets pressed with 16:1 stearic acid binder at 4 tons prior to sintering.

III. EDX analysis of as-synthesized $\text{CuFe}_{1-x}\text{Mg}_x\text{O}_2$

$\text{CuFe}_{1-x}\text{Mg}_x\text{O}_2$	Element	Atomic %
x=0	Cu	50 ± 2.5
	Fe	49 ± 2.5
x=0.0005	Cu	54 ± 2.7
	Fe	46 ± 2.3
x=0.005	Cu	49 ± 2.5
	Fe	51 ± 2.6
	Mg	0.5 ± 0.03
x=0.02	Cu	51 ± 2.6
	Fe	49 ± 2.5
	Mg	1 ± 0.05

Table S1: Quantification of Mg^{2+} content in $\text{CuFe}_{1-x}\text{Mg}_x\text{O}_2$ using EDX. Increasing Mg content was seen with increasing x value. For x=0.0005, the Mg content was below the detection limit of EDX, which is roughly 0.5%.

IV. XPS analysis of as-synthesized $\text{CuFe}_{1-x}\text{Mg}_x\text{O}_2$ at $x = 0$ and $x = 0.2$

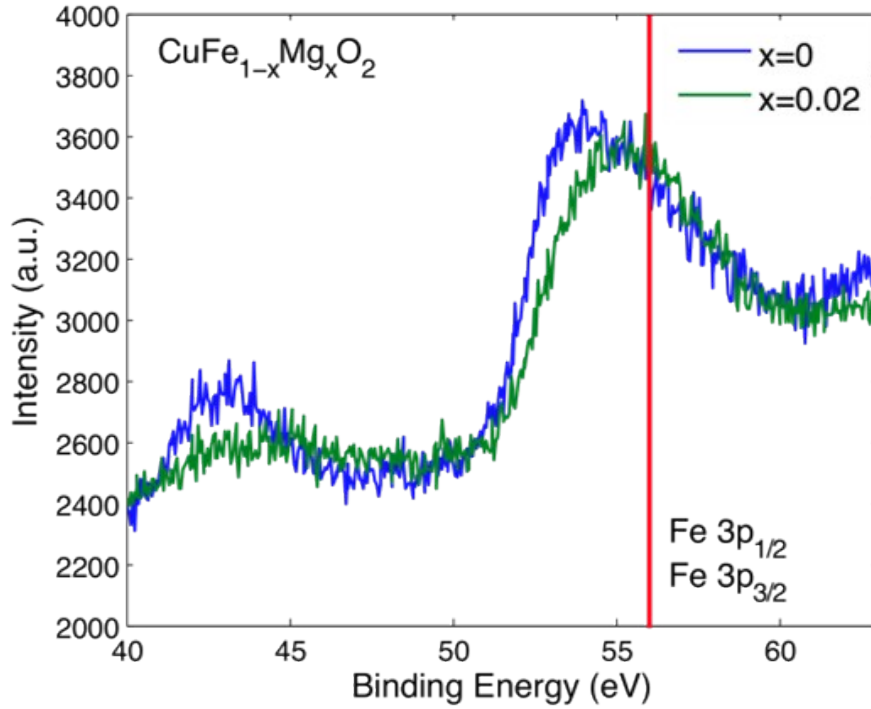


Figure S3: XPS spectra of undoped CuFeO_2 compared to the highest doped $\text{CuFe}_{1-x}\text{Mg}_x\text{O}_2$, $x=0.02$, sample. The absence of Mg 2s peak expected at 52 eV shows lack of Mg on the highest dopant sample surface, indicating the dopant is distributed in the bulk of the material (more than 2nm deep into the sample, i.e. beyond the surface sensitivity depth of XPS technique limited by inelastic mean free path of electrons). The 2eV peak shift may be related to the defect chemistry of the compounds due to doping, resulting in band bending effects, and more thorough investigation must be done beyond the scope of this study [2].

V. Absorption Spectrum of as-synthesized CuFeO₂

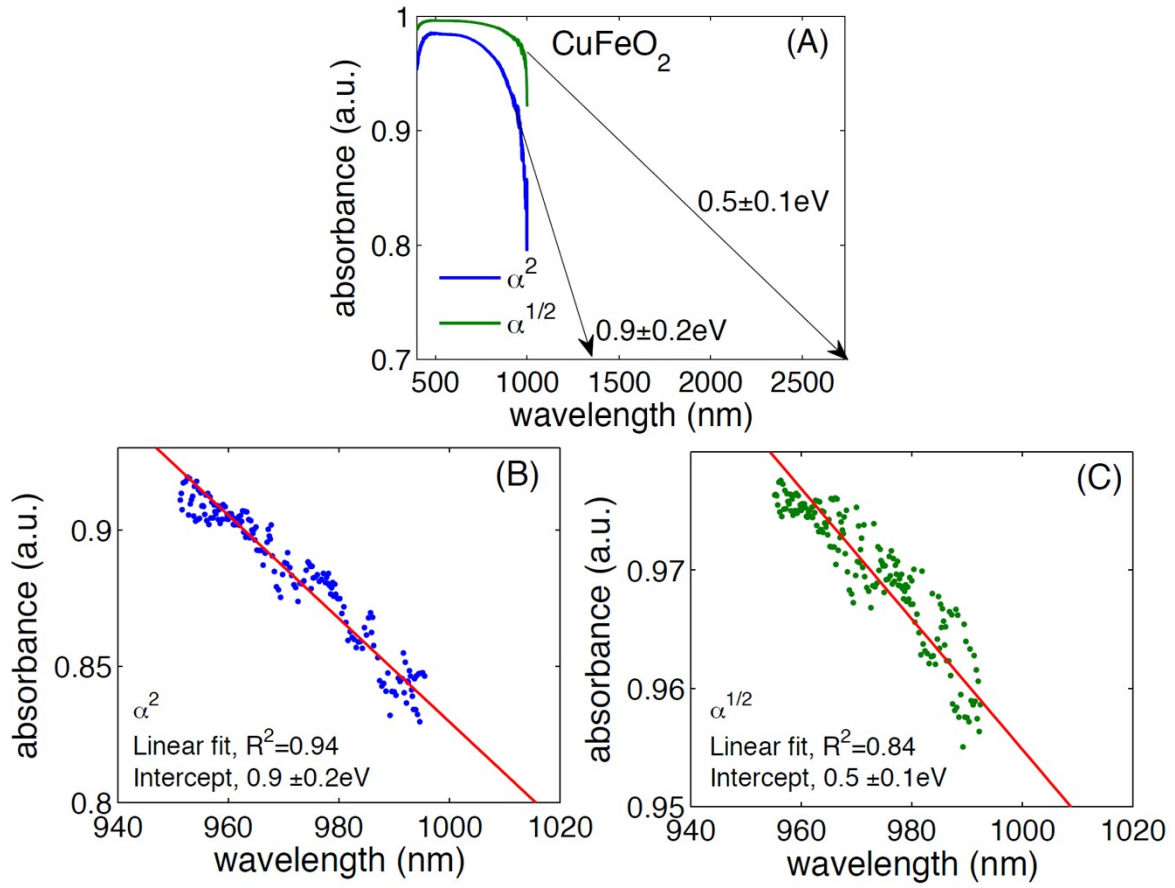


Figure S4. (A) UV-Vis-NIR absorption spectrum of CuFeO₂ yields an optical direct band gap of $0.9 \pm 0.2 \text{ eV}$ and an indirect band gap of $0.5 \text{ eV} \pm 0.1 \text{ eV}$ by extrapolation of the absorbance edge. Extrapolation is indicated with a black line, as a guide of the eye, and fit of the linear portion of the absorbance are presented in figures (B) for the direct band gap and (C) for the indirect band gap.

CuFeO₂ UV-Vis-NIR spectrum was obtained using a Horiba Lab Ram Aramis Spectrometer in reflection mode equipped with a Newport 6653 light source. A flat Ag mirror, yielding $\geq 99\%$ reflectivity in the visible and NIR range, was used as the internal standard, and the dark current was determined from a measurement performed in the absence of light and attributed to the detector noise. Assuming negligible optical transmission, reflected light from the sample was directly correlated to sample absorption, using the relationship,

$$A = 1 - R = 1 - \frac{SR - DC}{IS - DC}$$

(*A*- the sample absorbance, *R* - the reflectivity, *SR* - the sample reflection, *DC* - the dark current, *IS* - the internal standard).

VI. SEM and EDX analysis of a CuFeO_2 pellet post linear sweep voltammetry under chopped light illumination

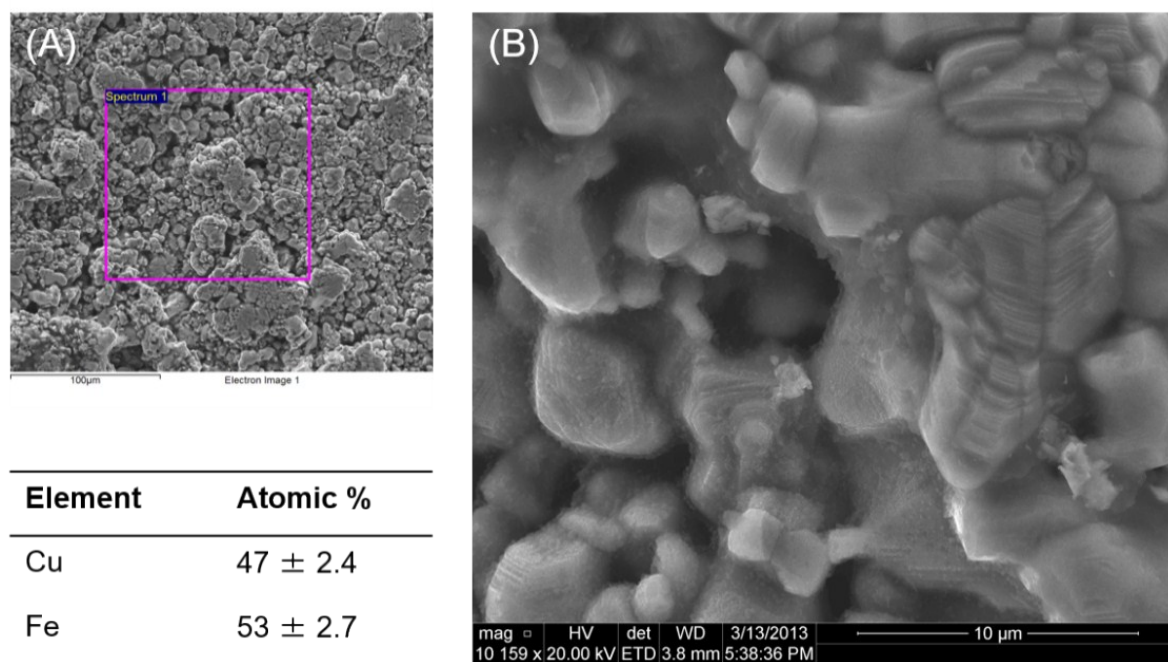


Figure S5: SEM and EDX analyses of CuFeO_2 pellets after use as a photocathode in a photoelectrochemical experiment. (A) Cu:Fe ratio is roughly 1:1. (B) SEM image after electrolysis.

VII. Flat Band Potential of $\text{CuFe}_{1-x}\text{Mg}_x\text{O}_2$ at $x = 0.005$

AC impedance data used to generate Mott-Schottky plots were collected in the dark using the same photoelectrochemical cell (PEC) as for photocurrent density experiments: (1) Au-sputtered $\text{CuFe}_{1-x}\text{Mg}_x\text{O}_2$ as the working electrode; (2) SCE as the reference; (3) a Pt mesh counter electrode; and (4) 0.1 M NaHCO_3 as the electrolyte. The data was collected using a CHI760 electrochemical workstation operating at 5 kHz and 100 kHz, employing a DC potential range from -0.3 to 0.6V with a 5mV peak-to-peak AC potential perturbation. Based on the Mott-Schottky equation,

$$\frac{1}{C^2} = \frac{2}{\epsilon\epsilon_0 A^2 e N_A} \left(V - V_{fb} - \frac{k_B T}{e} \right)$$

(C - capacitance associated with the space charge layer, A - interfacial area, N_A - number of acceptors, V - applied voltage, V_{fb} - flat band potential, k_B - Boltzmann's constant, T - absolute temperature, e - electronic charge), a linear plot of C^{-2} versus V is obtained, whose intercept yields V_{fb} . The interfacial capacitance term was found by measuring the bias-dependent impedance of the electrode assuming a simple equivalent circuit model, which accounts for the space charge layer capacitance at the solid-liquid interface in series with the uncompensated cell resistance.

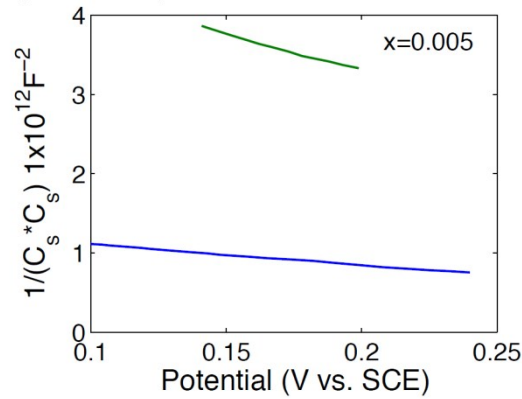


Figure S6. Mott-Shottky plot for $\text{CuFe}_{1-x}\text{Mg}_x\text{O}_2$ at $x = 0.005$ between 0.1 to 0.25 V vs. SCE collected at 5 (blue) and 10 (green) kHz. The flat band energy value was calculated via linear regression to estimate the x-intercept of the plot. The intercept value shows AC frequency-independent behavior.

A linear correlation between $\frac{1}{C^2}$, where C is the capacitance of the space charge layer, was found for $x = 0.005$. The data shown in Figure 2 was gathered at two frequencies, 5kHz and 10 kHz to ascertain whether the measured value of the capacitance is frequency dependent or not.

Extrapolation to the abscissa yields the flat band potential, which was measured to be 0.5 ± 0.1 V vs. SCE for $x=0.005$. This V_{fb} value is consistent with the values obtained in our previous work on the $\text{CuFe}_{1-x}\text{Mg}_x\text{O}_2$ system within experimental error.[1] Under the assumption that the host band structure does not change with dopant, it is expected that the V_{fb} would not vary.

VIII. Comparing synthesis of $\text{CuFe}_{1-x}\text{Mg}_x\text{O}_2$ with $\text{Cu}_{1-3x}\text{Mg}_x\text{FeO}_2$

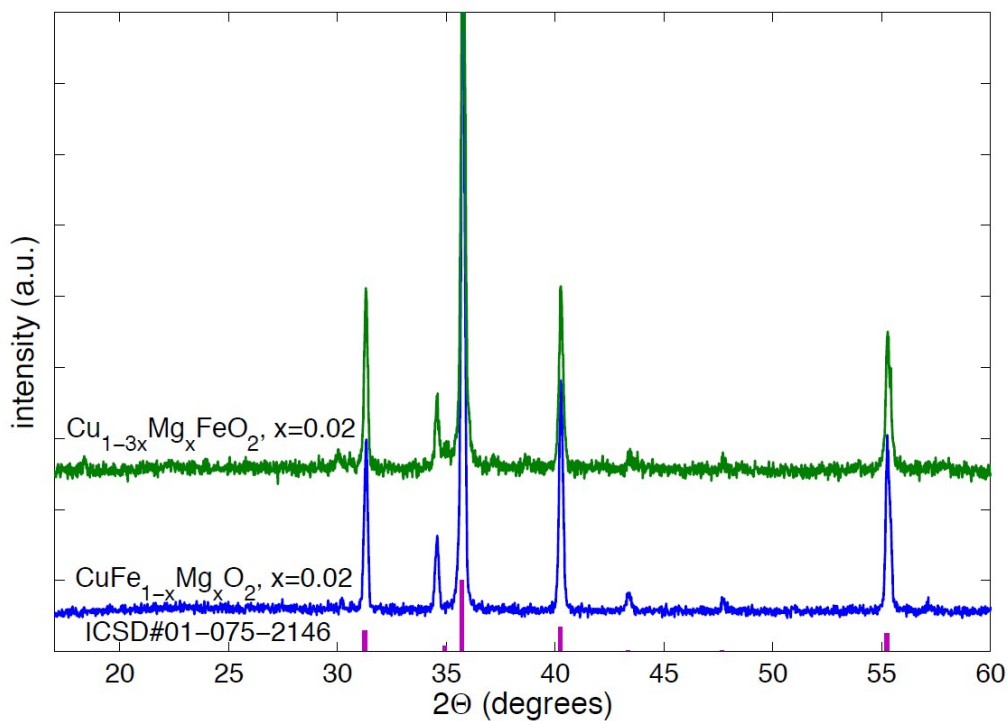


Figure S7. Comparing the synthesis of $\text{CuFe}_{1-x}\text{Mg}_x\text{O}_2$ with $\text{Cu}_{1-3x}\text{Mg}_x\text{FeO}_2$. XRD taken in powder form. $\text{CuFe}_{1-x}\text{Mg}_x\text{O}_2$ was synthesized at 850°C in Ar, and $\text{Cu}_{1-3x}\text{Mg}_x\text{FeO}_2$ was synthesized at the same temperature for 96 hours with intermittent grinding.

IX. Fe_3O_4 Impurity Phase in $\text{Cu}_{1-3x}\text{Mg}_x\text{FeO}_2$ for $x > 0.02$

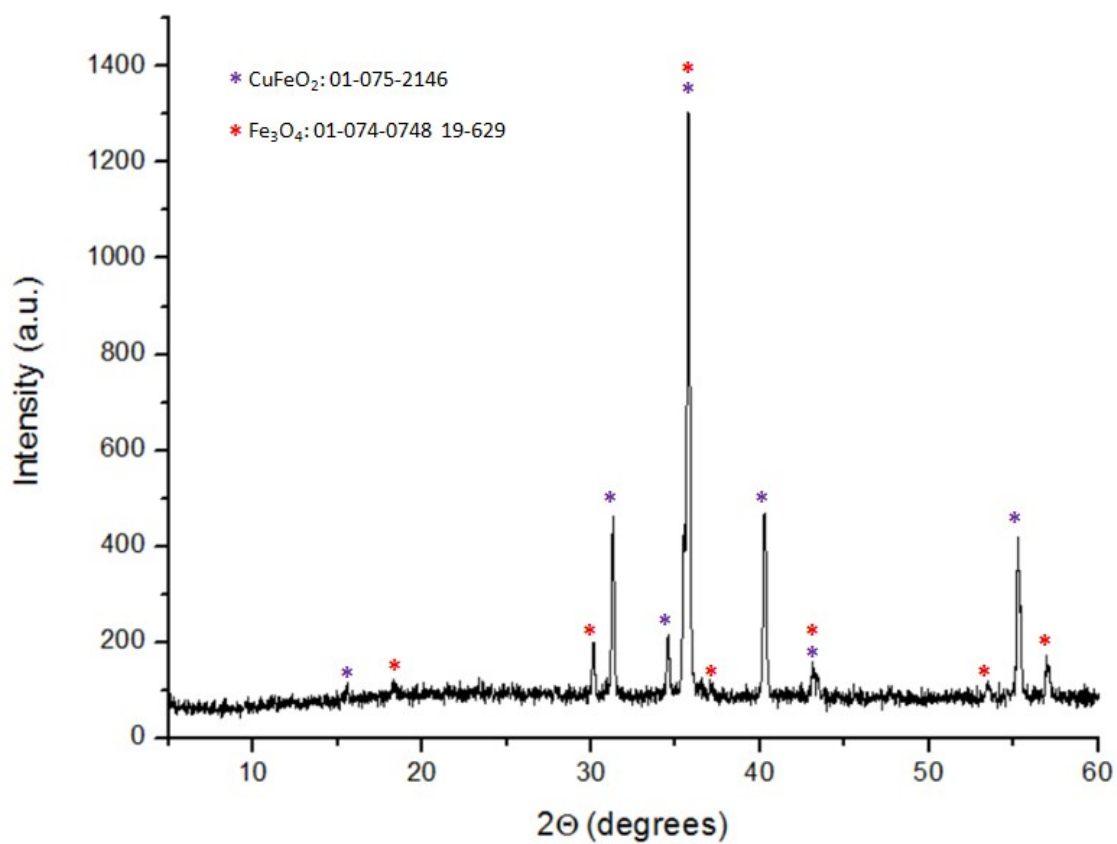


Figure S8. CuFeO_2 phase (purple) mixed with an Fe_3O_4 impurity phase (red) in the dopant series $\text{Cu}_{1-3x}\text{Mg}_x\text{FeO}_2$ at $x = 0.05$.

X. References

- [1] J. Gu, A. Wuttig, J. W. Krizan, *et al.*, *J. Phys. Chem. C*., **2013**, *117*, 12415–12422.
- [2] H. Sezen and S. Suzer, *J. Chem. Phys.*, **2011**, *135*, 141102.